

FROM HEAD TO TAIL: 3D IMAGING THE WHOLE-BODY MORPHOLOGY OF THE STEM GNATHOSTOME *ANGLASPIS HEINTZI*

LISA SCHNETZ, ^{1*}, AGNESE LANZETTI, ^{1,2}, ANDY S. JONES, ^{1,3}, RICHARD P. DEARDEN, ^{1,4}
STEPHAN LAUTENSCHLAGER, ^{1,3}, SAM GILES, ^{1,2}, ZERINA JOHANSON, ² and IVAN J. SANSOM ¹

¹School of Geography, Earth & Environmental Sciences, University of Birmingham, Edgbaston, Birmingham B15 2TT, U.K.,
l.schnetz@bham.ac.uk;

²Natural History Museum, Cromwell Road, London SW7 5BD, U.K.;

³Lapworth Museum of Geology, Birmingham B15 2TT, U.K.;

⁴Naturalis Biodiversity Center, Darwinweg 2, Leiden, 2333 CR, the Netherlands

ABSTRACT—Stem-gnathostomes are pivotal in reconstructing the evolutionary history of vertebrates but three-dimensional data of their body anatomies are currently lacking. Heterostracans, which constitute one of the earliest-branching lineages of stem-gnathostomes, present an ideal group to fill this gap as they are more commonly and completely preserved than other ostracoderm groups. Here, we reconstruct the first three-dimensional whole-body morphology of the cyathaspid heterostracan *Anglaspis heintzi*, using X-ray computed microtomography. The oral apparatus is composed of three oral plate pairs, one pair of lateral oral plates, and bounded by a pair of lateral plates. The trunk is formed of a series of heavily ornamented trunk, dorsal ridge, ventral ridge, and ventrolateral scales leading to the ‘hypocercal’ tail fin composed of numerous tail scales. Our retrodeformed reconstruction reveals a rigid oral apparatus incapable of substantial movement, resulting in a short wide gape to the mouth. This oral morphology precludes all previously proposed heterostracan feeding modes apart from suspension feeding. These findings contribute to the emerging consensus that heterostracans and jawless vertebrates more broadly possessed a greater diversity of feeding and swimming ecologies than previously thought.

SUPPLEMENTARY FILE(S)—Supplementary file(s) are available for this article for free at www.tandfonline.com/UJVP

Citation for this article: Schnetz, L., Lanzetti, A., Jones, A. S., Dearden, R. P., Lautenschlager, S., Giles, S., Johanson, Z., & Sansom, I. J. (2025) From head to tail: 3D imaging the whole-body morphology of the stem gnathostome *Anglaspis heintzi*. *Journal of Vertebrate Paleontology*. <https://doi.org/10.1080/02724634.2025.2476441>

Submitted: January 13, 2025

Revisions received: February 19, 2025

Accepted: February 24, 2025

INTRODUCTION

Stem-gnathostomes bridge the gap between living jawless (cyclostomes) and jawed vertebrates (crown-gnathostomes) and play a pivotal role in retracing the evolutionary origins of vertebrates. Dominating vertebrate assemblages from the Ordovician through to the early Devonian, they offer unique insights into the evolution of morphological disparity in the earliest members of the gnathostome lineage (e.g., Donoghue et al.,

2000; Ferrón et al., 2020; Keating & Donoghue, 2016). Most of these were heavily armored fish (‘ostracoderms’) and their rigid carapaces feature heavily in Paleozoic paleobiological, biostratigraphic and taxonomic studies (e.g., Ferrón & Donoghue, 2022; Janvier, 1996; Sallan et al., 2018). However, aside from their external head shields, detailed three-dimensional (3D) data on their body anatomies are mostly lacking, despite being key to new insights into feeding and locomotory strategies.

Heterostracans, one of the jawless stem-gnathostome groups, provide an ideal focal group to examine the evolution of vertebrate anatomy as their body regions are more commonly and completely preserved than any other ostracoderm group and they are often interpreted as one of the earliest branching lineages of stem-gnathostomes (Purnell, 2001; Sansom et al., 2015). The vast majority of heterostracan specimens/fossils are crushed and substantially disarticulated as well as encased in sediment which has, so far, hindered any in-depth visualization of the material. As a result, the existing literature is for the most part composed of traditional descriptions with magnified photos and interpretative drawings, on which reconstructions of the morphology are largely based. These reconstructions fail to include characterization of the detailed organization of the whole body (e.g., Denison, 1964), from which more accurate

*Corresponding author.

© 2025. Lisa Schnetz, Agnese Lanzetti, Andy S. Jones, Richard P. Dearden, Stephan Lautenschlager, Sam Giles, Zerina Johanson, Ivan J. Sansom.

This is an Open Access article distributed under the terms of the Creative Commons Attribution License (<http://creativecommons.org/licenses/by/4.0/>), which permits unrestricted use, distribution, and reproduction in any medium, provided the original work is properly cited. The terms on which this article has been published allow the posting of the Accepted Manuscript in a repository by the author(s) or with their consent.

Color versions of one or more of the figures in the article can be found online at www.tandfonline.com/ujvp.

interpretations of function can be drawn. Rare specimens are articulated (e.g., Blicek & Heintz, 1983; Broad & Dineley, 1973; Gross, 1963; Pernègre 2003; Soehn & Wilson, 1990; White, 1935) and may provide insights into heterostracan whole body anatomy but these interpretations are constrained by partial burial in the surrounding rock matrix. This masks important parts of the anatomy, which, in turn, hinders detailed full descriptions of specimens or analytical studies including morphometrics and consequent morphological variation analyses which were previously based on non-retrodeformed specimens (Ferrón et al., 2020; Gai et al., 2023).

Aside from the pteraspigid *Errivaspis* (Mark-Kurik & Botella, 2009; White, 1935), the whole-body morphology of heterostracans is best known in cyathaspidids (Denison, 1964). Within the Cyathaspididae, *Anglaspis* is the textbook representative and known from hundreds of isolated dorsal shields distributed around museum collections in North America and Europe (Blicek & Heintz, 1983). Three exceptionally preserved specimens of *Anglaspis heintzi* provided the basis for the whole-body illustrations of *Anglaspis* (Blicek & Heintz, 1983; Kiaer, 1932) but were limited to the morphology visible on the surface of the fossils. Using X-ray computed microtomography, these specimens provide a unique opportunity to study three-dimensionally preserved material and unlock the morphology of this archetypal cyathaspidid heterostracan. The main purpose of this study is to characterize and generate models of the head and tail regions of *Anglaspis heintzi* to reconstruct the first three-dimensionally articulated body of a heterostracan with all dermal elements arranged in life position. The reconstructions of these specimens allow for hypotheses for feeding and swimming in these early vertebrates to be tested and proposed/refined; as an example, 3D morphology of the oral region provides information about the size of the oral cavity, and the shape and function of the oral apparatus that closes this cavity.

MATERIALS AND METHODS

Specimens and Locality

Anglaspis heintzi (Blicek & Heintz, 1983) specimens PMO D382a-b and D384 are housed in the Natural History Museum in Oslo, Norway. Specimen PMO D382a-b consists of a single small block containing two articulated three-dimensional specimens of *Anglaspis heintzi*. The rostral regions of the specimens were cut and lost during historic collection of the block but the remaining head regions as well as the tails are preserved. Specimen PMO D384 includes the rostral portion of the three-dimensional head of one *Anglaspis heintzi* specimen. All specimens were collected from the lower Devonian outcrops of the Fraenkelryggen Formation (Red Bay Series, Lochkovian) in the northwest of Spitsbergen between 1909 and 1928 (Blicek & Heintz, 1983; Kiaer & Heintz, 1935). The Fraenkelryggen predominantly consists of fluvial deposits with some marine influences (Harland, 1997; Plotnick, 1999). Specimen PMO D384 was found in the *Prismaeva* horizon of the Fraenkelryggen Formation, while the horizon of PMO D382 is not known.

Terminology

There is a lack of consistency in the terminology applied to heterostracan oral anatomy. In order to stabilize this, we largely follow the terminology of Randle and Sansom (2017). For the anatomical axes of the animal as a whole we follow the terminology introduced by Dearden et al. (2024): we use dorsal/ventral in the dorsoventral axis, rostral/caudal for the sagittal axis, and dextral/sinistral for the transverse axis. When describing the oral plates, we use lateral/medial to describe lateral positions of the oral plates relative to the sagittal axis, ad/aboral to describe the surfaces of plates relative to the mouth, and proximal/distal

to refer to positions on the oral plates relative to their articulation with the ventral plate (proximal = near the ventral plate). Similarly, trunk and tail terminology in heterostracans and stem-gnathostomes is far from consistent, specifically with regards to the tail fin. Multiple terminologies have been adopted previously and are summarized in electronic supplementary material table S1. Here, we use ‘lobes’ to describe the subdivision of the tail fin, but do not differentiate the tail fin into dorsal/ventral lobes (fin ‘rays’ covered by larger scales that form the upper and lower portion of the tail) and digitations (intermediate fin ‘rays’ with smaller scales which support the fin web) as we observed no evidence for these as defined by Mark-Kurik and Botella (2009). For the trunk terminology, we largely follow Janvier (1996).

Computed Tomography

Anglaspis heintzi PMO D384 was scanned using a Nikon Metrology XTH 225ST X-ray CT machine fitted with a reflection target at the XTM Facility, Palaeobiology Research Group, University of Bristol. For D384, we first scanned the whole specimen, including the preserved caudal portions of the headshield (voltage: 100 kV, current: 169 μ A, 3141 projections, 1 frame, exposure: 1000 ms, no filtration, voxel resolution: 16.92 μ m, stack dimensions: 1610 X, 1588 Y, 1805 Z) (Fig. S1). We conducted a second scan targeting the orbital, oral, and pineal regions of the headshield (voltage: 85 kV, current: 142 μ A, 3141 projections, 2 frames, exposure: 1415 ms, no filtration, voxel resolution: 12.16 μ m, stack dimensions: 1860 X, 1772 Y, 1720 Z). Specimens PMO D382a-b were scanned using a Nikon Metrology XTH 225ST 2X X-ray CT machine at the Earth Sciences Department of the University of Birmingham. The whole block containing the two specimens was scanned with a rotating target (voltage: 100 kV, current: 380 μ A, 4181 projections, 2 frames, exposure: 708 ms, filtration: N/A, voxel resolution: 20.49 μ m, stack dimensions: 1248 X, 1905 Y, 2860 Z) (Fig. S5A). The resulting image stacks were initially processed in ImageJ 1.53o (Schneider et al., 2012) to crop the surrounding areas and improve contrast. A smoothing and Gaussian filter were also applied to PMO D384 to reduce noise. The stacks were segmented in Avizo 2021.1 (ThermoFisher Scientific) and Mimics v.23 (materialize) to visualize the 3D morphology. Reconstruction of PMO D384 was aimed at segmenting the individual plates and plate fragments to allow for retrodeformation. Therefore, the segmentation was performed manually using the paint brush and lasso tools with contrast thresholding every 10 slices and segmentation was completed via AI-assisted interpolation using the web-based application Biomedisa (Lösel et al., 2020). The inferred materials were then reimported to Avizo for manual check and refinement. Specimens PMO D382a-b were manually segmented using the thresholding, lasso, and livewire tools in Mimics v.23 (materialize) to extract the whole tail and fin structures as well as the articulation with the dorsal and ventral shield. The resultant 3D surface files were exported into and visualized in MeshLab 2022.02 (Cignoni et al., 2008) and Blender v. 3.4.1 (blender.org).

Reconstruction and Animation

Three-dimensional models of each segmented element or fragment of the *Anglaspis* specimens were imported into Blender for retrodeformation and rearticulation (version 3.0.0 for PMO D384; version 4.1 for PMO D382a-b). The retrodeformation process followed techniques detailed by Lautenschlager (2016) and Herbst et al. (2022). The morphology preserved in PMO D384 is affected by brittle deformation, resulting in cracks and disarticulation, rather than plastic deformation. Techniques used here were therefore limited to manual repositioning of elements; no techniques involved plastic alteration, rescaling or removal of preserved material. The tools used in Blender were

limited to rotation and translation to realign elements and the use of “Circle Select” followed by the “Mesh > Separate > Selection” sequence in Edit Mode to further separate segmented 3D surfaces along breaks to facilitate further realignment and more accurate reconstruction. Elements displaying the least displacement and those with clearly corresponding break facets or articulatory surfaces were realigned first, providing a robust basis for further rearticulation of elements. Next, elements with less clear articulations were repositioned with reference to element identifications and preserved positions in Blicek and Heintz (1983) and by the limits defined by the prior well-constrained retrodeformation. Retrodeformation in PMO D384 followed the sequence of: dorsal shield, ventral shield, branchial plates, suborbital plates, postoral plate, lateral plates, lateral-most oral plates, remaining medial oral plates. For the retrodeformation of the tail morphology, individual segmented elements of PMO D382a were used supplemented by information from PMO D382b. The process generally entailed the same steps as outlined above. The articulated elements of the caudalmost flank scales and the tail fin region were chosen as a starting point as these were in natural, in life articulation. Next, the flank scales were moved and rotated so that they overlapped as indicated by articulation facets identifiable by a break in ornamentation. In a similar style, the ventral scales were aligned with partial overlap in rostral direction. The width of the ventral scales provided a reference for the mediolateral position of the series of flank scales and, thereby, the overall body width. Apart from a caudalmost dorsal scale, which was articulated to the fin region, only one other disarticulated dorsal scale was preserved. This scale was duplicated and scaled to supplement the entire series of dorsal scales to articulate with the rostral most dorsal scale connecting to the head shield. The tail fin region, although mostly complete, contained some gaps at its caudal margin and showed moderate deformation. Using a lattice deform modifier in Blender, the tail fin was straightened and the missing portions filled in by duplicating and scaling parts of the preserved region to complete the outline. Given the mode of preservation, the exact margin of the fin region is not fully clear beyond a ‘hypocercal’ arrangement with the ventral part extending further than the dorsal part. The outline of the caudal margin is only indicative, though. In a final step, head and tail models were aligned to create the whole-body reconstruction. The most complete head shield elements in PMO D382a were duplicated and mirrored to create a bilaterally symmetrical complete composite for the reconstruction.

RESULTS

Head and Oral Region

PMO D384 consists of the rostral portion of the headshield of *Anglaspis heintzi*, from the oral region to just rostral to the branchial openings, encompassing about half of the total headshield length (Figs. 1A, S1). The ventral shield and oral region are visible on the surface, along with the margins of the lateral plates. The reconstruction further reveals the dorsal shield, the branchial and suborbital plates, and the remaining parts of the lateral plates which are all well-preserved in the matrix (Fig. 1B, C, E–G). The specimen was dorsoventrally flattened during diagenesis. The dorsal and ventral shields are fractured in large sections but retain their morphological margins (Fig. 1B, C). The dorsal and ventral shields of PMO D384 reveal similar characteristics to previous descriptions following the three-dimensional reconstruction, most notably the deep V-shaped ornamental ridges (Blicek & Heintz, 1983) (Figs. 1B, C, S2). The paired lateral branchial plates have thin but deep ornamental ridges that run rostro-caudally. The dorsal ridges converge towards the anteroventral side of the plate, following the

edge of the plate that forms a 30° angle (Fig. 1F, G). The paired suborbital plates sit on top of this angled margin (Fig. 1F, G). They also present ornamental ridges running rostro-caudally and accommodating the concave shape of the orbital margin. This plate likely corresponds to plate “Or(4)” in Blicek and Heintz (1983). The internal sides of the dorsal and ventral shields, branchial and suborbital plates are mostly smooth with some small pits (Fig. 1H).

The oral region includes three pairs of oral plates and a singular postoral plate and is bordered laterally by paired lateral oral plates (one per side) (Figs. 1D, S4). These correspond to plate “Or(3)” in previous descriptions (Blicek & Heintz, 1983) (Fig. S2A). The ornamental ridges of these plates run dorsoventrally at a 45° angle, with a lateral margin of the ventral plate dextrally and a smaller angle sinistrally. The lateral oral plates are more elongated rostro-caudally compared with the oral plates and terminate where the ventral and dorsal shields come to form the straight oral margins. The internal surface of all of these plates is smooth and does not appear to have any visible articulating surface, either laterally or proximally with the post-oral plate. The oral apparatus of PMO D384 is dextrally composed of three damaged small oral plate fragments and sinistrally of three more complete oral plates (Figs. 1C, D, S3). This differs from previous descriptions (Blicek & Heintz, 1983), which reconstructed only two large oral plates on either side (corresponding to “Or(2)” and “Or(1)”) (Fig. S2A). Based on the more complete sinistral side, the outermost oral plate (op 3) is larger than the others and triangular in shape (Fig. S3). The distal margin of op 3 follows the dorsal plate oral margin and tapers off medially. The two oral plates (op 1, op 2) medial to this are smaller and fragmentary, forming a somewhat triangular shape. The three oral plates on the dextral side are reconstructed here as more fragmentary when compared with the sinistral side.

The postoral plate, which corresponds to “Or(m)” in Blicek and Heintz (1983), is reconstructed as a comparatively reduced plate (Figs. 1D, S2A, S3). It has an equilateral triangular shape with a large proximal base and distal tip. The classification of this plate as a postoral plate is based on its position at the center of the mouth and its direct articulation onto the rostral margin of the ventral plate (Fig. 1H). The postoral plate is smooth on the adoral surface but shows prominent ornamental ridges on the aboral side which appear to extend beyond the caudal edge of the base. It exhibits steep ridges running along the distal and proximal edges of the plate perpendicular to the ornamental ridges, with the caudal facet shorter than the rostral one. The rostral ridges likely provided articulation surfaces for the oral plates. The caudal ridge is concave and matches the medial rostral indentation present at the leading edge of the ventral plate; in cross section the leading edge of the ventral shield is wrapped by a sulcus in the caudal margin of the postoral plate (Fig. 1H).

Tail

Specimens PMO D382a and PMO382b consist of two almost-complete specimens with nearly complete articulated tail trunk and tail fin (Figs. 2A, 4, S5A). The caudal halves of the head region, including the branchial openings, are preserved in both specimens but the suborbital and oral regions are not (Figs. 2B, S5B). The headshields are sufficiently well-preserved to identify the dorsal and ventral shield, and thus the orientation of the tail trunk and fin. The description here is based primarily on PMO D382a since it is better preserved (Fig. 2A), but descriptions of PMO D382b are added where appropriate (Fig. S5, Fig. 3). The dorsal side of the specimens is exposed from the matrix following preparations (Fig. S5A). Specimen PMO D382a is additionally exposed laterally at the edge of the block.

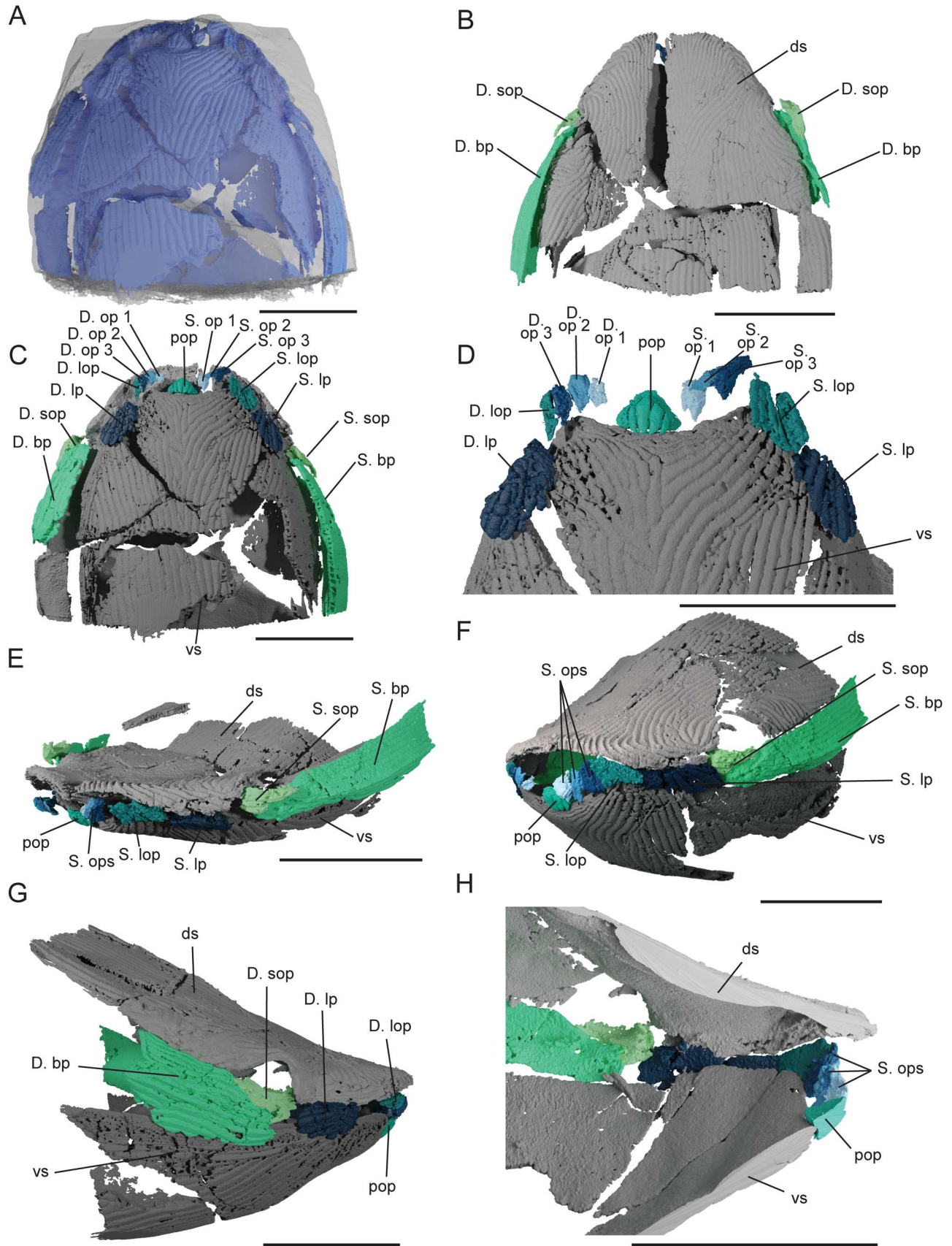


FIGURE 1. *Anglaspis heintzi* PMO D384 head region. **A**, specimen in situ; **B–E**, original rendering of head region based on computed tomographic data in **B**, dorsal; **C**, ventral; **D**, ventral close-up (dorsal and branchial material removed); **E**, sinistral rostral-lateral view; **F**, **G**, retrodeformed head region in **F**, sinistral rostral-lateral and **G**, dextral view; **H**, sagittal cross section showing articulation of the postoral plate and the ventral shield. **Abbreviations:** bp, branchial plate; D, dextral; ds, dorsal shield; lop, lateral oral plate; lp, lateral plate; op, oral plate; ops, oral plates; pop, postoral plate; S, sinistral; sop, suborbital plate; vs, ventral shield. Scale bars equal 0.5 cm.

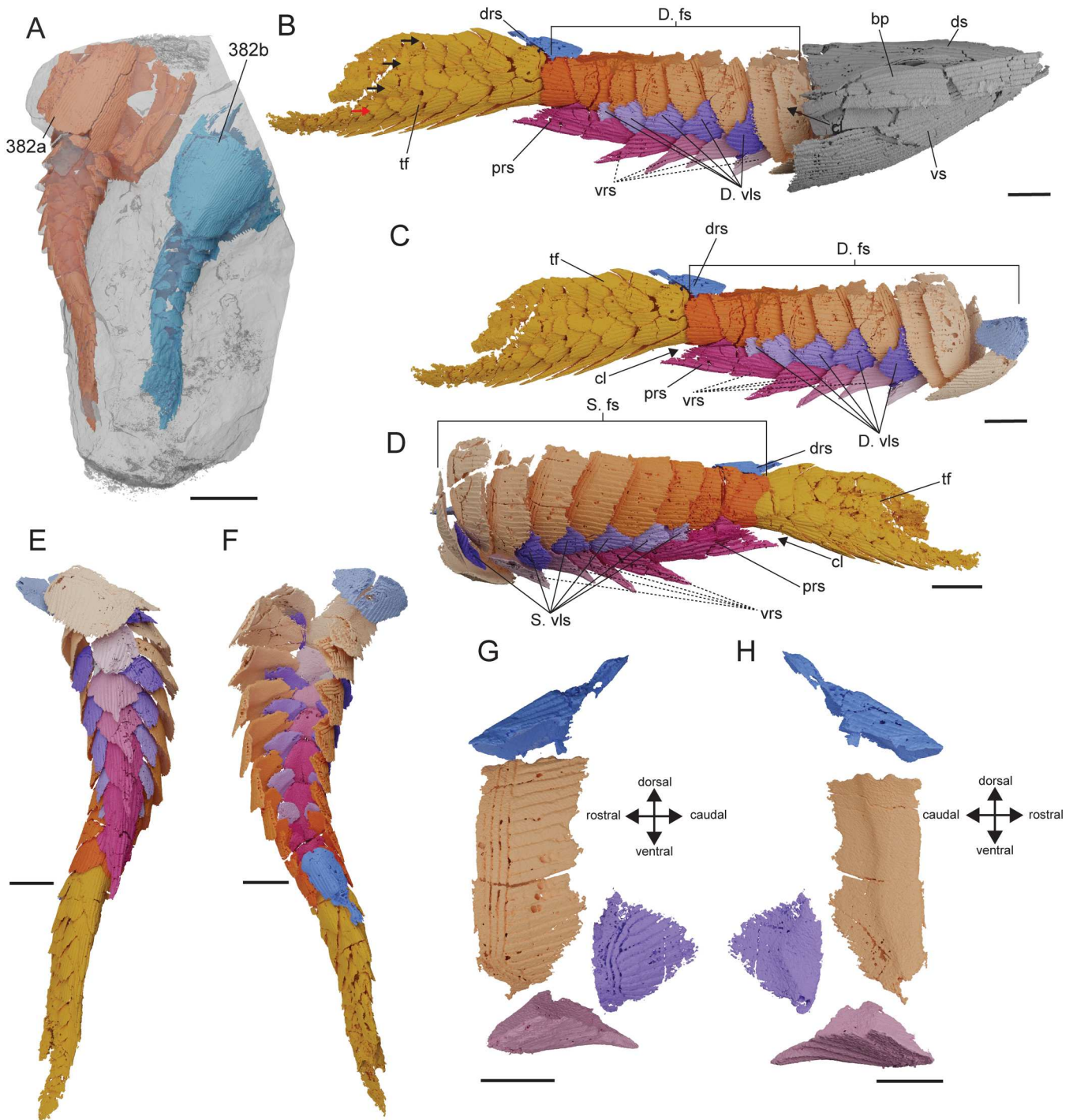


FIGURE 2. *Anglaspis heintzi* PMO D382a tail region. **A**, specimen in situ; **B–E**, original rendering of the tail region based on computed tomographic data in **B**, dextral including the head shield; **C**, dextral; **D**, sinistral; **E**, ventral; and **F**, dorsal view; **G**, **H**, sinistral dorsal, flank, ventrolateral, and ventral ridge scale in **G**, external and **H**, internal view; black arrows in **B** indicate positions of tail lobes, red arrow represents the ‘hypochordal’ lobe. **Abbreviations:** bp, branchial plate; cl, cloaca; **D**, dextral; **drs**, dorsal ridge scales; **ds**, dorsal shield; **fs**, flank scale; **prs**, preanal ridge scale; **S**, sinistral; **tf**, tail fin; **vls**, ventrolateral scales; **vrs**, ventral ridge scales; **vs**, ventral shield. Scale bar equals 1 cm in **A**, 3 mm in **B–F**, and 2 mm in **G** and **H**.

The tail trunk of PMO D382a is formed of nine dorsoventrally elongate paired plate segments (=flank scales), which do not connect to each other dorsally or ventrally (Figs. 2B–F, 4). Six smaller diamond-shaped ventrolateral scales are sandwiched in between the flank scales sinistrally (Figs. 2D, 4A)

and five ventrolateral scales dextrally (Figs. 2B–C, 4B). There is no ventrolateral scale between the first and second as well as second to third flank scale in the dextral series (Fig. 4B), while there is no ventrolateral scale between the second and third flank scale in the sinistral series (Fig. 4A). Based on

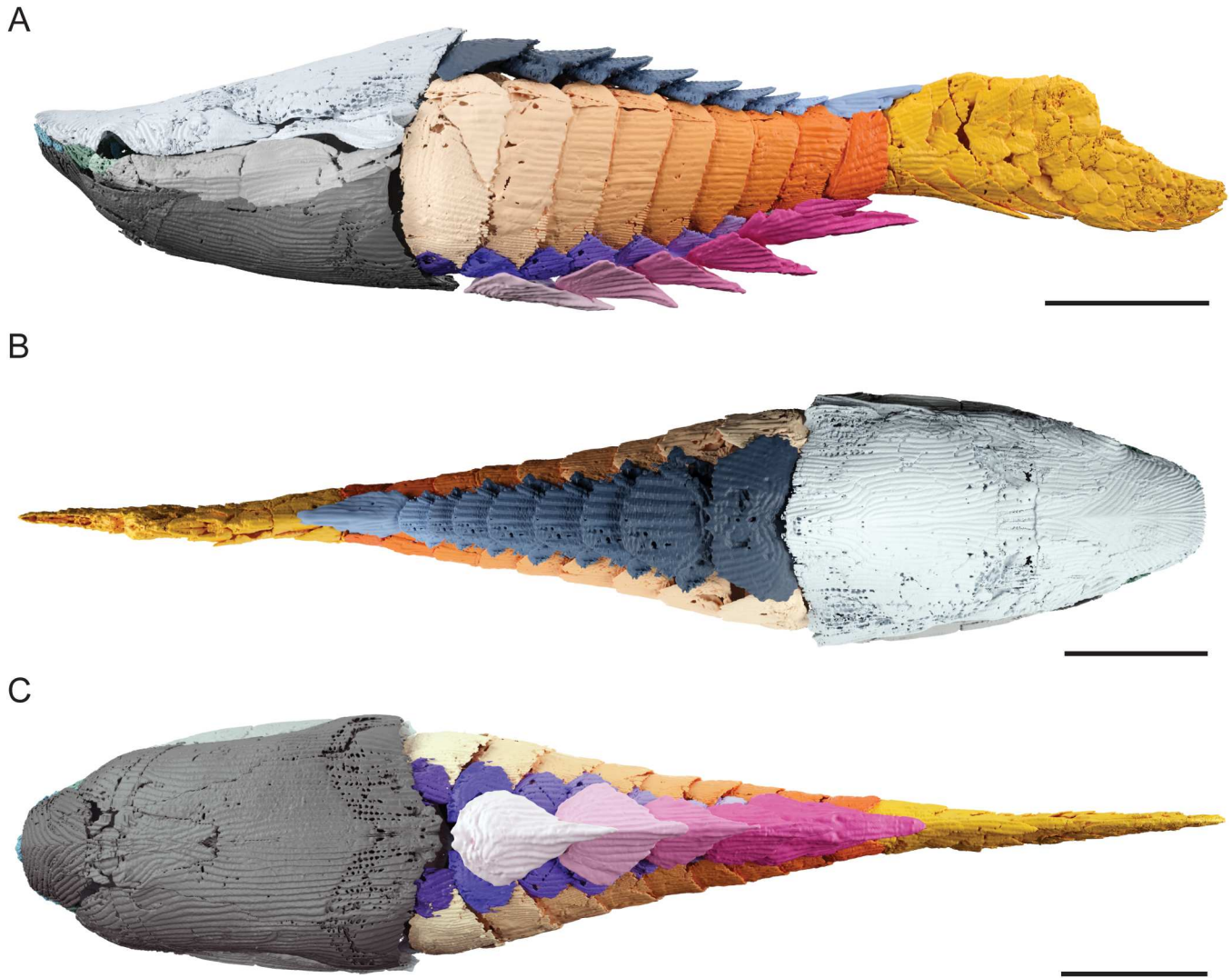


FIGURE 3. Reconstruction of *Anglaspis heintzi* based on specimens PMO D384 and PMO D382a-b combined. **A**, sinistral; **B**, dorsal; **C**, ventral view. Scale bars equal 1 cm.

the material presented here, we assume this to be a preservational absence. Specimen PMO D382b only preserves four ventrolateral scales on either side of the trunk, with no scales between the first three flank scales (Fig. S5). The flank scales of PMO D382a are bordered dorsally and ventrally by a singular series of smaller dorsal and ventral scales with spiny projections (Figs. 2B–F, 4). The dorsal scales, which represent the median dorsal ridge scales sensu Janvier (1996), are overlying the flank scales but only the caudalmost scale between the end of the tail trunk and the start of the tail fin is preserved in PMO D382a (Figs. 2B–D, 2F, 4, S6). The plate is triangular in shape and slightly elevated in the center, with a rostro-caudally elongated spine. Specimen PMO D382b preserves three complete dorsal ridge scales (the rostralmost and two caudalmost scales) as well as four dorsal ridge scale fragments, indicating a complete dorsal covering of the tail trunk (Fig. S5C, E). The rostralmost and caudalmost scales are shaped similarly to the one in PMO D382a. The third scale is shaped more square-like and slightly concave in the center but does not adorn a rostro-caudally elongated spine (Fig. S5C, E). The diagonal of the square is rostro-caudally aligned.

The ventral scales represent a complete series of five smaller plates that are preserved filling the gap between the flank scales and the ventrolateral scales (Figs. 2B–E, Fig. 3A, C, 4). Like the dorsal ridge scales, they possess rostro-caudal projections that form a spinose structure. The first four scales have been termed preanal ridge scales, while the fifth is referred to as the postanal plate by Janvier (1996). The position of the anus/cloaca in our reconstruction of *Anglaspis* would have been after the fifth ventral scale, the only position to support an opening. Therefore, the first four ventral scales are here referred to as ventral ridge scales and the fifth one as preanal ridge scale. The spines of the ventral ridge scales have an angle of about 20° from the main axis that slightly increases towards the caudal scales. The spine of the preanal scale is almost parallel to the main axis as shown by the rostro-caudal orientation of the ornament and sits at the end of the tail trunk where it connects to the tail fin (Fig. 3A). It underlaps the more caudal scales considerably and its shape relative to the more caudal scales creates a gap in the squamation for the cloaca. The ornamentation of the flank, dorsal, ventrolateral, and ventral scales consist of ridges running

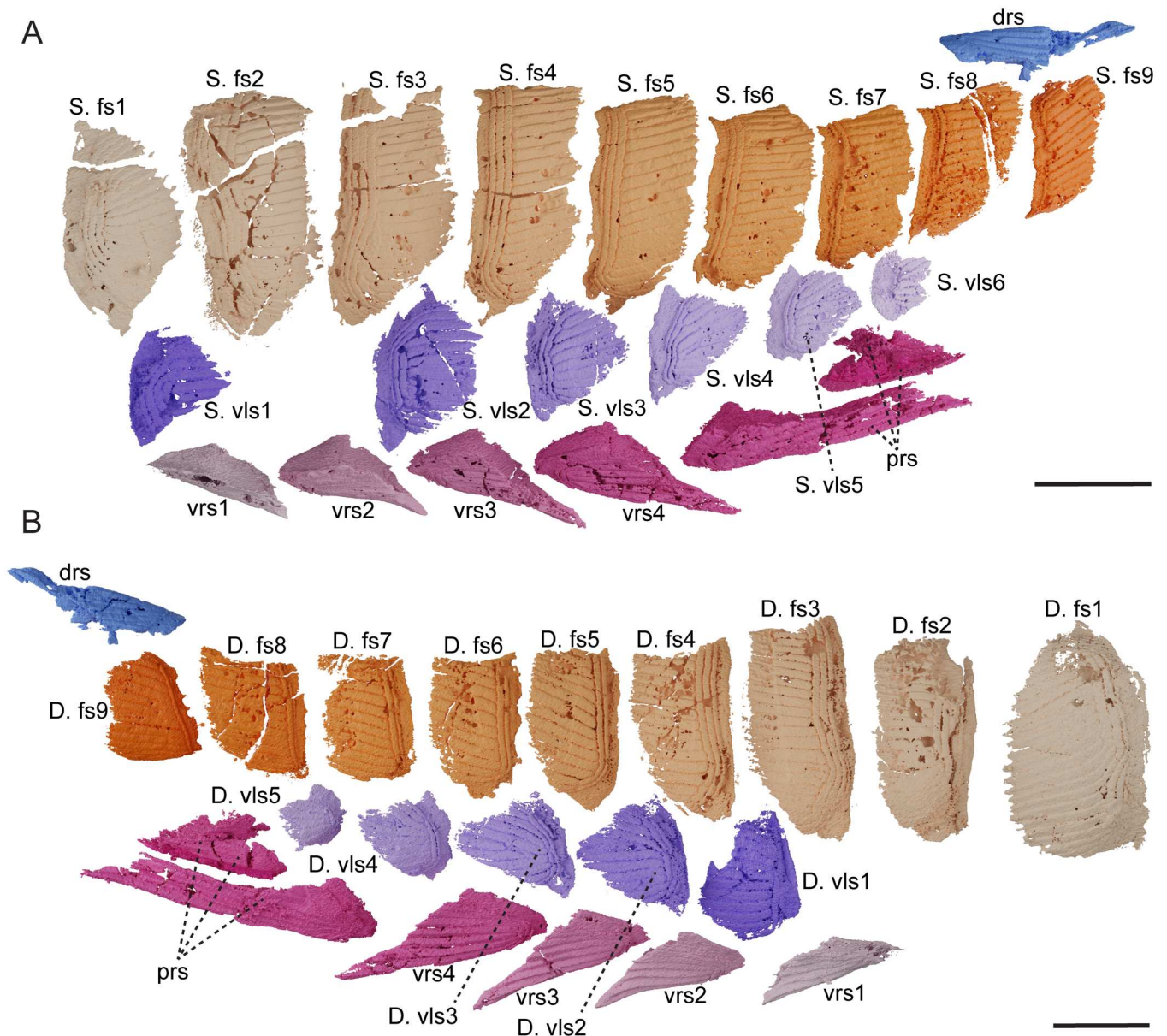


FIGURE 4. *Anglaspis heintzi* PMO D382a reconstructed trunk squamation, including flank, dorsal ridge, ventrolateral, and ventral scales. **A**, sinistral lateral view; **B**, dextral lateral view. **Abbreviations:** D, dextral; drs, dorsal ridge scales; fs, flank scale; prs, preanal ridge scale; S, sinistral; vls, ventrolateral scales; vrs, ventral ridge scales. Scale bars equal 3 mm.

rostro-caudally (Figs. 2G, 4). The flank and ventrolateral scales additionally exhibit comparatively subdued dorsoventrally oriented ridges on their leading/rostral edge. The internal surfaces of the flank segments are overall smooth but show a thickening of the medial region at about two-thirds of the rostro-caudal length (Fig. 2H). The rostral position of the segments (rostral to the ridge) is thicker than the caudal position. This likely represents the articular region between the individual segments and is also visible in PMO D382b.

The tail fin of PMO D382a is complete and composed of at least 25 small square and rounded paired flat scales tightly fitted together on each side to form the tail shape (Fig. 2B–D). The tail fin is laterally compressed and subdivided into four lobes (Fig. 2B, see also Table S1 for further details on terminology), with the ventral lobe extending the furthest caudally (Fig.

2B–F). The ventral scales that border the tail fin are unpaired and have elongated triangular spines running rostro-caudally. The tail fin scales exhibit a wrinkled ornament but still preserve the rostro-caudal dentine ridges seen in the trunk scale ornamentation. The caudal end of the tail fin is not completely intact but outlines the overall ‘hypocercal’ tail shape (prominent ventral lobe and shorter dorsal lobe). The extension of the notochord into the lower lobe of the tail cannot be confirmed from the fossilized evidence.

DISCUSSION

The three-dimensional data and revision to the anatomy of *Anglaspis heintzi* we present here have a number of implications

for the paleobiological interpretation of this fish, as well as heterostracans (and ostracoderms) more broadly.

Oral Apparatus and Feeding Ecologies

Previous reconstructions of *Anglaspis* and cyathaspids more generally have proposed considerable rotation of the oral and postoral plates (by $\sim 55^\circ$) based upon the same material (Bendix-Almgreen, 1986). The fragmentary preservation of the oral plates in PMO D384 makes inferring their exact movements difficult. However, the articulation surfaces on the rostral edge of the postoral plate suggest the oral plates may have been partially articulating with it but also may have expanded outwards at an angle around it as seen in *Rhinopteraspis* (Dearden et al., 2024). The postoral plate, in contrast, is solidly anchored to the ventral shield, and substantial movement of the former is not possible given the shape of the articular surface (Fig. 1H). Reconstructions of (somewhat) mobile oral plates relative to an immobile postoral plate have also recently been highlighted in the pteraspidiiform *Rhinopteraspis* (Dearden et al., 2024), suggesting that this morphology might be more widespread in heterostracans. What is clear, though, is that the plates in *Anglaspis* were smaller and more numerous than reconstructed by Blicke and Heintz (1983).

The resulting buccal cavity delimited by the ventral and dorsal shield would have formed an ellipse as is presented in the reconstruction, with the oral plates limiting but not completely occluding the rostral opening of the mouth. Any potential movement of the oral plates would have aided in regulation of the oral aperture and might have permitted an increase of water influx to the oral cavity. The oral morphology of *Anglaspis heintzi* as presented here is overall congruent with a microphagous suspension feeding strategy and supports previous hypotheses on heterostracan feeding ecologies (Dearden et al., 2024; Purnell, 2002). Another feeding strategy commonly hypothesized for heterostracans is deposit feeding, with the fish scooping sediment and food particles from the sea floor (White, 1935). This requires significant movement of the oral plates aided by movement of the postoral plate and can be rejected based on our reconstruction of the oral apparatus of *Anglaspis*: movement of the postoral plate is severely limited in PMO D384. In addition, *Anglaspis* exhibits strong ornamentation on the ventral surface of its body as well as prominent ventral spines, all of which would have likely been subjected to considerable wear upon repeated contact with the seafloor. Our retrodeformed whole body reconstruction furthermore demonstrates a body shape inconsistent with the flat-bottomed body arrangement of demersal ostracoderms (Fig. 3) (i.e., osteostracans, galeaspids [Janvier, 1996]). Thus, the absence of wear and demersal body shape also supports rejection of a detritus feeding ecology (Denison, 1973; Purnell, 2002). Hypotheses of a predatory feeding mode in heterostracans have been previously discussed in detail and rejected (Dearden et al., 2024; Grohgan et al., 2024a; Purnell, 2002), and we cannot find any morphological evidence (i.e., firm biting surface, occlusion mechanism, and approach angle of the oral plates with the dorsal shield) for such an ecology in *Anglaspis*. Cyathaspids specifically were previously suggested to be macrophagous feeders capable of a scraping motion (Bendix-Almgreen, 1986), which can be rejected based on our findings as it would have required considerable outward movement of the postoral and oral plates and visible wear on these plates.

The morphology and arrangement of the oral plates and the resulting size and shape of the oral cavity in *Anglaspis heintzi* is difficult to compare with other cyathaspids due to the widespread lack of detailed information on the 3D morphology of the latter. From the 2D information available, cyathaspid oral systems range from a single plate in *Poraspis* (Elliott & Petriello, 2011) to multiple-plated structures in taxa such as *Capitaspis*

(Elliott & Petriello, 2013) and *Allocryptaspis* (Elliott et al., 2004); *Anglaspis* also shows the multi-plated morphology (as presented here). Outside of the cyathaspids, heterostracan oral morphologies are best known in the pteraspidiiform clade (Dearden et al., 2024; fig. 5; Grohgan et al., 2023, 2024a, b). Oral plate morphologies and numbers conform more closely in pteraspidiiforms, consisting of multiple pairs of elongated, finger-like oral plates with a caudal alignment of a hook-like structure (e.g., *Rhinopteraspis* [Dearden et al., 2024; fig. 5], *Mylopteraspidella* [Stensiö, 1964], *Protopteraspis* [Kiaer, 1928], and *Errivaspis* [White, 1935]). However, this is not universal as varied morphologies are found within the group in taxa such as *Drepanaspis* (Gross, 1963) and *Doryaspis* (Pernègre, 2003), indicating some disparity in feeding structures. *Athenaegis*, which constitutes the oldest articulated heterostracan known to date, is regularly placed as an outgroup to both cyathaspids and pteraspids (Elliott et al., 2021; Randle & Sansom, 2016, 2017). The oral apparatus of *Athenaegis* has been interpreted previously as pteraspid-like, comprising a series of finger-like plates arranged in a fan-like structure (Soehn & Wilson, 1990). The oral structures of tessellate and problematic heterostracans, which fall outside of cyathaspids, *Athenaegis*, and pteraspidiiforms, are currently unknown. A framework for comparing homologies of individual plates in heterostracans, specifically cyathaspids and pteraspids, is lacking and difficult to establish (see Elliott et al. [2021] and Randle & Sansom [2017] for the most recent phylogenetic analyses). Moreover, among these varied taxa, only the oral apparatus of *Rhinopteraspis* has been investigated in 3D, with only minor ability of plate movement resulting in a restricted mouth gape (Dearden et al., 2024).

Trunk Squamation in Heterostracans and Stem-Gnathostomes

The data of *Anglaspis* presented here provide the best-characterized record of an articulated trunk and tail squamation in a heterostracan. Few trunk squamations are known in heterostracans; those that are preserved fall into one of two broad categories, which may be phylogenetically informative. The first of these can be seen in *Errivaspis waynensis*, one of the most widely illustrated pteraspidiiforms, which has diamond-shaped body scales and dorsal and ventral rows of enlarged median scales (White, 1935). This pattern appears to be fairly conserved in pteraspidiiforms including *Doryaspis* (Pernègre, 2003), *Protaspis*, *Lampraspis*, and *Cardipeltis* (Denison, 1971) and is also present in *Athenaegis* (Soehn & Wilson, 1990). In contrast, in the second of these categories, the flank squamation of cyathaspids instead tends to comprise larger rod-shaped scales as seen in *Anglaspis* (Fig. 4), although with some variation in organization (e.g., *Nahanniaspis*, *Dinaspidella*, *Torpedaspis* [Broad & Dineley, 1973; Dineley & Loeffler, 1976]). In tessellate heterostracans such as *Lepidaspis*, the body squamation comprises tesserae distinct from those of the head and also includes median ridge scales (Dineley & Loeffler, 1976). *Anglaspis* shows that heterostracan flank scales had specialized overlap surfaces, identifiable by abrupt termination of the ornamental ridges, although nothing as complex as the scale pegs identified in mandibulate gnathostomes (Cui et al., 2019, 2023, 2025). Although the morphology of the scales is variable, a commonality of these heterostracan trunk squamations are dorsal and ventral rows of spinose median ridge scales that continue along the dorsal and ventral edges of the tail (Denison, 1971).

More broadly, stem-gnathostome trunk squamation is variable and seems unlikely to carry a phylogenetic signal (Gai et al., 2023). Osteostracans have rod shaped flank scales of variable lengths, dorsal scutes associated with fins and ventrolateral ridge scales (Janvier, 1985; Ritchie, 1967; White & Toombs, 1983). Rare articulated galeaspids have small diamond-shaped flank-scales and dorsal scutes (Gai et al., 2022, 2023). Thelodonts

are microsquamous with no evidence for enlarged ridge scales (e.g., Märss & Ritchie, 1997), while anaspids have highly patterned splint-shaped scales (e.g., Blom, 2012). Mandibulate stem-gnathostomes have smaller plate-shaped scales, and also have scutes associated with the dorsal and ventral midlines including fins (Wang & Zhu, 2022; Cui et al., 2023). Commonalities within these include median rows of scutes, which in more crownward taxa become associated with dorsal fins (Gai et al., 2022; White & Toombs, 1983; Wang & Zhu, 2022). Specialized areas surrounding the anal vent are present in *Anglaspis* and galeaspids, *Tujiaspis* (Gai et al., 2022), and in mandibulate stem-gnathostomes (Cui et al., 2023).

Comparisons of Tail Anatomy in Stem Gnathostomes

The tail of *Anglaspis* is reconstructed in this study as being four-lobed and asymmetrical with the ventral lobe larger than the dorsal lobes and extending caudally. This confirms most previous reconstructions of *Anglaspis* (Blieck & Heintz, 1983; Denison, 1971; Janvier, 1996; Kiaer, 1932) but rejects others that suggested a ‘trilobated’ tail (Blieck & Heintz, 1983). However, although an extension of the notochord into the lower ‘hypochordal’ lobe of the tail seems likely, the absence of soft tissue anatomy prevents confirmation of this diagnostic feature of hypocercal tail morphology (Denison, 1971, but see discussion in Mark-Kurik & Botella, 2009). A ‘hypocercal’ tail has been considered as present in most heterostracans but a variety of tail morphologies have been documented, including near symmetrical ‘forked’ forms (Pellerin & Wilson [1995] in the irregulariaspid cyathaspids *Nahannaspis* and *Dinaspidella*; Denison [1966, 1971] in *Cardipeltis*) and digitated asymmetrical forms (Mark-Kurik & Botella [2009] in *Errivaspis*).

The distribution of tail morphologies within stem-gnathostomes has been the subject of much discussion (e.g., Gai et al., 2023; Pradel et al., 2007), although many of these broader treatments adopt a single morphology as being representative of the whole group, obscuring the variation that is evident within heterostracans. Assumptions of such uniformity influence body shape and subsequent morphological variation analyses (e.g., Ferrón et al., 2020), as well as swimming abilities (Denison, 1971; Ferrón & Donoghue, 2022). The ‘hypocercal’ tail of *Anglaspis* was likely an adaptation to allow for a significant lift to occur with forward motion, facilitating movement away from the sea-floor in the absence of paired fins (Denison, 1971; Kermack, 1943), and again contrary to hypotheses of detritus-feeding. Recent analyses have additionally shown that the cephalic shield in pteraspidiiform heterostracans enhances vortex lift forces during forward swimming, comparable to delta wings, allowing for better exploitation of the water column (Botella et al., 2024). Gai et al. (2023) used a ‘hypocercal’ condition for ‘pteraspidiomorphs’ (= in part to heterostracans) and estimated their swimming speed to fall in among other groups of jawless armored fishes such as the Anaspidia and Galeaspidia.

Tail structure seems to carry clearer phylogenetic signal than trunk squamation in early vertebrates. Hypocercal tails, where, as noted, the notochord deflects into the ventral lobe, are present in galeaspids (Gai et al., 2022, 2023), some thelodonts (Märss & Ritchie, 1997), anaspids (e.g., Blom, 2012), *Sacabambaspis* (Pradel et al., 2007), as well as some heterostracans. Hypercercal tails (with the notochord extending into the dorsal lobe) are present in all known mandibulate gnathostomes (e.g., *Coccoosteus* Miles & Westoll, 1968) and osteostracans, which seems to reflect a clear phylogenetic transition (Pradel et al., 2007). It has been suggested that unusual diphyccercal tails in some heterostracans and thelodonts (Pellerin & Wilson, 1995; Wilson & Caldwell, 1993) represent an intermediary between these (Pradel et al., 2007). Phylogenetic bracketing (following the evolutionary hypothesis of Reeves et al., 2023) and the

presence of hypocercal tails with digitations in the more derived galeaspids (Gai et al., 2022, 2023) suggest that these diphyccercal tails are more likely modifications of the hypocercal condition.

CONCLUSION

The majority of studies on the anatomy of stem-gnathostomes have largely relied on inferences from compressed and largely two-dimensional fossils. Using X-ray computed microtomography and retrodeformation techniques, we have reconstructed the whole-body anatomy of the cyathaspid heterostracan *Anglaspis heintzi*, offering a new perspective on the three-dimensional bauplan of stem-gnathostomes. The oral apparatus of *Anglaspis heintzi* is composed of three pairs of oral plates, one postoral plate, one pair of lateral oral plates and bounded by one pair of lateral plates. A reduced postoral plate supports an articulation of the oral plates. Our retrodeformed reconstruction reveals a narrow gape of the mouth, with the oral structures capable of limited movement. Out of the previously proposed feeding modes for heterostracans, our new data exclude all but a suspension feeding style, similar to the pteraspid *Rhinopteraspis* (Dearden et al., 2024). The tail of *Anglaspis heintzi* is formed of a series of heavily ornamented trunk, dorsal ridge, ventral ridge, and ventrolateral scales preceding a four-lobed ‘hypocercal’ tail fin, which in itself is composed of more than 25 scales on either side. The ‘hypocercal’ tail of *Anglaspis heintzi* allowed for lift during forward motion in the absence of paired fins, supporting a suspension feeding mode. Our results highlight the importance of high-resolution CT-scanning for allowing new and detailed visualizations of the morphology of these key fossils in the evolution of vertebrate anatomy. These also unlock future research directions such as functional analyses to test various feeding mode hypotheses, including range of motion (ROM) and computational fluid dynamics (CFD). The findings presented here contribute to the emerging consensus that heterostracans exhibited a far greater disparity of their whole-body anatomies than previously thought, highlighting that feeding and swimming ecologies were already diverse in these early vertebrates.

ACKNOWLEDGMENTS

We thank M. Purnell (University of Leicester) for highlighting these specimens to us and further discussion on heterostracan feeding. We also want to thank M. Grohgan and P. Donoghue for debates surrounding heterostracan feeding. Many thanks to J.H. Hurum and Ø. Hammer for access to the collections of the Universitet i Oslo Naturhistorisk Museum. We thank L. Martin-Silverstone (University of Bristol) for help with CT-scanning of PMO D384. The authors would also like to thank E. Randle for discussions on heterostracan phylogeny. This work is funded by the Leverhulme Trust (RPG-2021-271 ‘Feeding without jaws: innovations in early vertebrates’). R.P. Dearden is supported by funding from the European Union’s Horizon Europe research and innovation program under the Marie Skłodowska-Curie grant agreement No. 101062426. S. Giles was supported by a Royal Society Dorothy Hodgkin Research Fellowship (no. DH160098).

AUTHOR CONTRIBUTIONS

SG, SL, ZJ, and IJS conceptualized the work. LS, AL, ASJ, RD, SL, and SG segmented and visualized the data. ASJ and SL retrodeformed the 3D models. LS, AL, ASJ, RD, SG, and IJS analyzed the data. LS, AL, ASJ, RD, and IJS wrote the paper. SL, SG, and

ZJ contributed to reviewing and editing the paper. All authors gave final approval for publication.









DATA AVAILABILITY STATEMENT

All data are available in the main text or supplementary data attached to this publication. The datasets, including the 3D models and raw CT data, are on the Zenodo data repository (<https://doi.org/10.5281/zenodo.14051800>).

DISCLOSURE STATEMENT

No potential conflict of interest was reported by the author(s).

ORCID

Lisa Schnetz  <http://orcid.org/0000-0002-7504-2614>
 Agnese Lanzetti  <http://orcid.org/0000-0003-1364-0544>
 Andy S. Jones  <http://orcid.org/0000-0002-9118-5965>
 Richard P. Dearden  <http://orcid.org/0000-0003-3522-7304>
 Stephan Lautenschlager  <http://orcid.org/0000-0003-3472-814X>
 Sam Giles  <http://orcid.org/0000-0001-9267-4392>
 Zerina Johanson  <http://orcid.org/0000-0002-8444-6776>
 Ivan J. Sansom  <http://orcid.org/0000-0003-3043-8989>

SUPPLEMENTARY FILE(S)

Supplementary Figures 1–6 and Supplementary Table 1.

LITERATURE CITED

- Bendix-Almgreen, S. E. (1986). Silurian ostracoderms from Washington Land (North Greenland), with comments on cyathaspid structure, systematics and phyletic position. *Rapport Grønlands Geologiske Undersøgelse*, 132, 89–123. <https://doi.org/10.34194/rapgu.v132.7970>
- Blieck, A., & Heintz, N. (1983). The cyathaspids of the Red Bay Group (Lower Devonian) of Spitsbergen. *Polar Research*, 1(1), 49–74. doi:10.1111/j.1751-8369.1983.tb00731.x.
- Blom, H. (2012). New birkenioid anaspid from the Lower Devonian of Scotland and its phylogenetic implications. *Palaeontology*, 55(3), 641–652. <https://doi.org/10.1111/j.1475-4983.2012.01142.x>.
- Botella, H., Fariña, R. A., & Huera-Huarte, F. (2024). Delta wing design in earliest nektonic vertebrates. *Communications Biology*, 7(1), 1153. <https://doi.org/10.1038/s42003-024-06837-8>
- Broad, D. S., & Dineley, D. L. (1973). *Torpedaspis*, a new upper Silurian and Lower Devonian genus of Cyathaspididae (Ostracodermi) from arctic Canada. *Geological Survey of Canada, Bulletin*, 222, 53–91. <https://doi.org/10.4095/102368>
- Cignoni, P., Callieri, M., Corsini, M., Dellepiane, M., Ganovelli, F., & Ranzuglia, G. (2008). MeshLab: an Open-Source Mesh Processing Tool. *ERCIM News*, 2008, 45–46. <https://doi.org/10.2312/LocalChapterEvents/ItalChap/ItalianChapConf2008/129-136>.
- Cui, X., Friedman, M., Yu, Y., Zhu, Y.-a., & Zhu, M. (2023). Bony-fish-like scales in a Silurian maxillate placoderm. *Nature Communications*, 14(1), 7622. <https://doi.org/10.1038/s41467-023-43557-9>
- Cui, X., Qiao, T., Peng, L., & Zhu, M. (2025). New material of the Early Devonian sarcopterygian *Styloichthys changae* illuminates the origin of cosmine. *Journal of Systematic Palaeontology*, 23(1). <https://doi.org/10.1080/14772019.2024.2432273>
- Cui, X., Qiao, T., & Zhu, M. (2019). Scale morphology and squamation pattern of *Guiyu oneiros* provide new insights into early osteichthyan body plan. *Scientific Reports*, 9(1), 4411. <https://doi.org/10.1038/s41598-019-40845-7>
- Dearden, R., Jones, A., Giles, S., Lanzetti, A., Grohgan, M., Johanson, Z., Lautenschlager, S., Randle, E., Donoghue, P. C. J., & Sansom, I. J. (2024). The three-dimensionally articulated oral apparatus of a Devonian heterostracan sheds light on feeding in Palaeozoic jawless fishes. *Proceedings of the Royal Society B: Biological Sciences*, 291(2019), 20232258. <https://doi.org/10.1098/rspb.2023.2258>
- Denison, R. H. (1964). The Cyathaspididae; a family of Silurian and Devonian jawless vertebrates. *Fieldiana Geology*, 13, 309–473.
- Denison, R. H. (1966). *Cardipeltis*, an early Devonian agnathan of the order Heterostraci. *Fieldiana Geology*, 16, 89–116.
- Denison, R. H. (1971). On the tail of the Heterostraci (Agnatha). *Forma et function*, 4, 87–99.
- Denison, R. H. (1973). Growth and wear of the shield in Pteraspidae (Agnatha). *Palaeontographica, Abteilung A*, 143, 1–10.
- Dineley, D. L., & Loeffler, E. J. (1976). Ostracoderm faunas of the Delorme and associated Siluro-Devonian Formations, North West Territories, Canada. *Special Papers in Palaeontology*, 18, 1–214.
- Donoghue, P. C. J., Forey, P. L., & Aldridge, R. J. (2000). Conodont affinity and chordate phylogeny. *Biological Reviews*, 75(2), 181–251. <https://doi.org/10.1111/j.1469-185X.1999.tb00045.x>
- Elliott, D. K., Lassiter, L., & Blieck, A. (2021). A phylogenetic analysis of the Cyathaspididae (Vertebrata: Pteraspido-morphi: Heterostraci). *Acta Palaeontologica Polonica*, 66(3), 631–640. <https://doi.org/10.4202/app.00811.2020>
- Elliott, D. K., & Petriello, M. A. (2011). New poraspids (Agnatha, Heterostraci) from the Early Devonian of the western United States. *Journal of Vertebrate Paleontology*, 31(3), 518–530. <https://doi.org/10.1080/02724634.2011.557113>
- Elliott, D. K., & Petriello, M. A. (2013). A new cyathaspid (Agnatha, Heterostraci) with an articulated oral cover from the Late Silurian of the Canadian Arctic. *Journal of Vertebrate Paleontology*, 33(1), 29–34. <https://doi.org/10.1080/02724634.2012.717568>
- Elliott, D. K., Reed, R. C., & Loeffler, E. J. (2004). A new species of *Alloctypaspis* (Heterostraci) from the Early Devonian, with comments on the structure of the oral area in cyathaspids. In G. Arratia, M. V. H. Wilson, & R. Cloutier (Eds.), *Recent advances in the origin and early radiation of vertebrates* (pp. 455–472). Verlag Dr. Friedrich Pfeil.
- Ferrón, H. G., Greenwood, J. M., Deline, B., Martínez-Pérez, C., Botella, H., Sansom, R. S., Ruta, M., & Donoghue, P. C. J. (2020). Categorical versus geometric morphometric approaches to characterizing the evolution of morphological disparity in Osteostraci (Vertebrata, stem Gnathostomata). *Palaeontology*, 63(5), 717–732. <https://doi.org/10.1111/pala.12482>
- Ferrón, H. G., & Donoghue, P. C. J. (2022). Evolutionary analysis of swimming speed in early vertebrates challenges the ‘New Head Hypothesis’. *Communications Biology*, 5(1), 863. <https://doi.org/10.1038/s42003-022-03730-0>
- Gai, Z., Li, Q., Ferrón, H. G., Keating, J. N., Wang, J., Donoghue, P. C. J., & Zhu, M. (2022). Galeaspid anatomy and the origin of vertebrate paired appendages. *Nature*, 609(7929), 959–963. <https://doi.org/10.1038/s41586-022-04897-6>
- Gai, Z., Lin, X., Shan, X., Ferrón, H. G., & Donoghue, P. C. J. (2023). Postcranial disparity of galeaspid and the evolution of swimming speeds in stem-gnathostomes. *National Science Review*, 10(7), nwad050. <https://doi.org/10.1093/nsr/nwad050>
- Grohgan, M., Ballell, A., Rayfield, E. J., Ferrón, H. G., Johanson, Z., & Donoghue, P. C. J. (2024a). Finite element and microstructural analyses indicate that pteraspid heterostracan oral plate microstructure was adapted to a mechanical function. *Palaeontology*, 67(6), e12733. <https://doi.org/10.1111/pala.12733>
- Grohgan, M., Ferrón, H. G., Johanson, Z., & Donoghue, P. C. J. (2023). Testing hypotheses of pteraspid heterostracan feeding using computational fluid dynamics. *Journal of Vertebrate Paleontology*, 43(2), e2272974. <https://doi.org/10.1080/02724634.2023.2272974>
- Grohgan, M., Johanson, Z., Keating, J. N., & Donoghue, P. C. J. (2024b). Morphogenesis of pteraspid heterostracan oral plates and the evolutionary origin of teeth. *Royal Society Open Science*, 11(12), 240836. <https://doi.org/10.1098/rsos.240836>
- Gross, W. (1963). *Drepanaspis gemundenensis* Schlüter Neuuntersuchung. *Palaeontographica, Abteilung A*, 121, 133–155.
- Harland, W. B. (1997). Chapter 16 Devonian history. In W. B. Harland (Ed.), *The geology of Svalbard* (pp. 289–309). Geological Society Memoir No. 17.
- Herbst, E. C., Meade, L. E., Lautenschlager, S., Fioritti, N., & Scheyer, T. M. (2022). A toolbox for the retrodeformation and muscle reconstruction of fossil specimens in Blender. *Royal Society Open Science*, 9(8), 220519. <https://doi.org/10.1098/rsos.220519>
- Janvier, P. (1985). *Les Cephalaspides du Spitsberg*. Cahiers de Paléontologie, Editions du C.N.R.S.

- Janvier, P. (1996). *Early vertebrates*. Clarendon Press.
- Keating, J. N., & Donoghue, P. C. J. (2016). Histology and affinity of anaspids, and the early evolution of the vertebrate dermal skeleton. *Proceedings of the Royal Society B: Biological Sciences*, 283(1826), 20152917. <https://doi.org/10.1098/rspb.2015.2917>
- Kermack, K. A. (1943). The functional significance of the hypocercal tail in *Pteraspis rostrata*. *Journal of Experimental Biology*, 20(1), 23–27. <https://doi.org/10.1242/jeb.20.1.23>.
- Kiaer, J. (1928). The structure of the mouth of the oldest known vertebrates, pteraspids and cephalaspids. *Palaeobiologica*, 1, 117–134.
- Kiaer, J. (1932). The Downtonian and Devonian vertebrates of Spitsbergen, IV. Suborder Cyathaspida. *Skrifter om Svalbard og Ishavet*, 52, 1–26.
- Kiaer, J., & Heintz, A. (1935). The Downtonian and Devonian vertebrates of Spitsbergen, V. Suborder Cyathaspida I: tribe Poraspidei, family Poraspidae. *Skrifter om Svalbard og Ishavet*, 40(40), 1–138.
- Lautenschlager, S. (2016). Reconstructing the past: methods and techniques for the digital restoration of fossils. *Royal Society Open Science*, 3(10), 160342. <https://doi.org/10.1098/rsos.160342>
- Lösel, P. D., van de Kamp, T., Jayme, A., Ershov, A., Faragó, T., Pichler, O., Tan Jerome, N., Aadepe, N., Bremer, S., Chilingaryan, S. A., Heethoff, M., Kopmann, A., Odar, J., Schmelzle, S., Zuber, M., Wittbrodt, J., Baumbach, T., & Heuveline, V. (2020). Introducing Biomedisa as an open-source online platform for biomedical image segmentation. *Nature Communications*, 11(1), 5777. <https://doi.org/10.1038/s41467-020-19303-w>
- Märss, T., & Ritchie, A. (1997). Articulated thelodonts (Agnatha) from Scotland. *Transactions of the Royal Society of Edinburgh: Earth Sciences*, 88(3), 143–195. <https://doi.org/10.1017/S026359330000691X>.
- Mark-Kurik, E., & Botella, H. (2009). On the tail of *Errivaspis* and the condition of the caudal fin in heterostracans. *Acta Zoologica*, 90(s1), 44–51. <https://doi.org/10.1111/j.1463-6395.2008.00355.x>.
- Miles, R. S., & Westoll, T. S. (1968). The placoderm fish *Coccosteus cuspidatus* Miller ex Agassiz from the Middle Old Red Sandstone of Scotland. Part 1. Descriptive morphology. *Transactions of the Royal Society of Edinburgh*, 67(9), 373–476. <https://doi.org/10.1017/S0080456800024078>.
- Pellerin, N. M., & Wilson, M. V. H. (1995). New evidence for structure of Irregulariaspididae tails from Lochkovian beds of the Delorme Group, Mackenzie Mountains, Northwest Territories, Canada. *Geobios*, 28, 45–50. [https://doi.org/10.1016/S0016-6995\(95\)80085-9](https://doi.org/10.1016/S0016-6995(95)80085-9)
- Pernègre, V. N. (2003). The genus *Doryaspis* White (Heterostraci) from the Lower Devonian of Vestspitsbergen, Svalbard. *Journal of Vertebrate Paleontology*, 22(4), 735–746. [https://doi.org/10.1671/0272-4634\(2002\)022\[0735:TGDWHF\]2.0.CO;2](https://doi.org/10.1671/0272-4634(2002)022[0735:TGDWHF]2.0.CO;2).
- Plotnick, R. E. (1999). Habitat of Llandoveryan-Lochkovian eurypterids. In A. J. Boucot, & J. D. Lawson (Eds.), *Paleocommunities - a Case Study from the Silurian and Lower Devonian* (pp. 106–136). Cambridge University Press.
- Pradel, A., Sansom, I. J., Gagnier, P.-Y., Cespedes, R., & Janvier, P. (2007). The tail of the Ordovician fish *Sacabambaspis*. *Biology Letters*, 3(1), 73–76. <https://doi.org/10.1098/rsbl.2006.0557>
- Purnell, M. A. (2001). Scenarios, selection, and the ecology of early vertebrates. In P. E. Ahlberg (Ed.), *Major events in vertebrate evolution* (pp. 187–208). Taylor and Francis.
- Purnell, M. A. (2002). Feeding in extinct jawless heterostracan fishes and testing scenarios of early vertebrate evolution. *Proceedings of the Royal Society of London. Series B: Biological Sciences*, 269(1486), 83–88. <https://doi.org/10.1098/rspb.2001.1826>
- Randle, E., & Sansom, R. S. (2016). Exploring phylogenetic relationships of Pteraspidoformes heterostracans (stem-gnathostomes) using continuous and discrete characters. *Journal of Systematic Palaeontology*, 15(7), 583–599. <https://doi.org/10.1080/14772019.2016.1208293>.
- Randle, E., & Sansom, R. S. (2017). Phylogenetic relationships of the ‘higher heterostracans’ (Heterostraci: Pteraspidoformes and Cyathaspididae), extinct jawless vertebrates. *Zoological Journal of the Linnean Society*, 181(4), 910–926. <https://doi.org/10.1093/zoolinnean/zlx025>.
- Reeves, J. C., Wogelius, R. A., Keating, J. N., & Sansom, R. S. (2023). *Lasanius*, an exceptionally preserved Silurian jawless fish from Scotland. *Palaeontology*, 66(2), e12643. <https://doi.org/10.1111/pala.12643>.
- Ritchie, A. (1967). *Ateleaspis tessellata* Traquair, a non-cornuate cephalaspid from the Upper Silurian of Scotland. *Journal of the Linnean Society of London, Zoology*, 47(311), 69–81. <https://doi.org/10.1111/j.1096-3642.1967.tb01396.x>.
- Sallan, L., Friedman, M., Sansom, R. S., Bird, C. M., & Sansom, I. J. (2018). The nearshore cradle of early vertebrate diversification. *Science*, 362(6413), 460–464. doi: 10.1126/science.aar3689.
- Sansom, R. S., Randle, E., & Donoghue, P. C. J. (2015). Discriminating signal from noise in the fossil record of early vertebrates reveals cryptic evolutionary history. *Proceedings of the Royal Society B: Biological Sciences*, 282(1800), 20142245. <https://doi.org/10.1098/rspb.2014.2245>
- Schneider, C. A., Rasband, W. S., & Eliceiri, K. (2012). NIH Image to ImageJ: 25 years of image analysis. *Nature Methods*, 9(7), 671–675. <https://doi.org/10.1038/nmeth.2089>
- Soehn, K. L., & Wilson, M. V. H. (1990). A complete, articulated heterostracan from Wenlockian (Silurian) beds of the Delorme Group, Mackenzie Mountains, Northwest Territories, Canada. *Journal of Vertebrate Paleontology*, 10(4), 405–419. <https://doi.org/10.1080/02724634.1990.10011825>.
- Stensiö, E. (1964). Les Cyclostomes fossiles ou Ostracodermes. In J. Piveteau (Ed.), *Traité de paléontologie* (pp. 96–383). Masson.
- Wang, Y., & Zhu, M. (2022). Squamation and scale morphology at the root of jawed vertebrates. *eLife*, 11, e76661. <https://doi.org/10.7554/eLife.76661>
- White, E. I. (1935). The ostracoderm *Pteraspis* Kner and the relationships of the agnathous vertebrates. *Philosophical Transactions of the Royal Society of London. Series B, Biological Sciences*, 225, 381–456. <https://doi.org/10.1098/rstb.1935.0015>
- White, E. I., & Toombs, H. A. (1983). The cephalaspids from the Dittonian section at Cwm Mill, near Abergavenny, Gwent. *Bulletin of the British Museum (Natural History) Geology*, 37, 149–171.
- Wilson, M. V. H., & Caldwell, M. W. (1993). New Silurian and Devonian fork-tailed “thelodonts” and jawless vertebrates with stomachs and deep bodies. *Nature*, 361(6411), 442–444. <https://doi.org/10.1038/361442a0>

Handling Editor: Carole Burrow.